AN IMPLICIT DISCONTINUOUS GALERKIN FINITE ELEMENT METHOD FOR WATER WAVES

J. J. W. van der Vegt, V. R. Ambati, O. Bokhove
Department of Applied Mathematics, University of Twente, Enschede, The Netherlands
Email: j.j.w.vandervegt@math.utwente.nl

Abstract

We discuss a new higher order accurate discontinuous Galerkin finite element method for non-linear free surface gravity waves. The algorithm is based on an arbitrary Lagrangian Eulerian description of the flow field using deforming elements and a moving mesh, which makes it possible to represent non-linear large amplitude waves. The novel feature of the algorithm is a coupled treatment of the free surface boundary condition and the domain discretization, which improves numerical stability.

Introduction

The numerical simulation of free surface gravity waves is an essential tool in the design and analysis of wave motion and its influence on fixed and floating structures. Free surface gravity waves can be modelled at various levels of sophistication, but for many applications it is sufficient to consider waves in an inviscid, incompressible and irrotational flow. This makes it possible to introduce a potential function satisfying the Laplace equation together with a non-linear free surface boundary condition.

Despite this significant mathematical simplification one still has to face a number of challenging numerical problems. In particular, maintaining numerical stability and robustness for schemes with minimal dispersion and dissipation errors is non-trivial. This applies both to boundary integral and finite element methods.

In this paper we will discuss a new implicit and higher order accurate discontinuous Galerkin (DG) finite element discretization which does not suffer from a frequently encountered weak, mesh dependent saw-tooth type instability at the free surface. This discontinuous Galerkin algorithm combines the well known benefits of a local, element wise discretization suitable for efficient *hp*-mesh adaptation and parallel computing with an unconditionally stable numerical discretization, which maintains accuracy on non-smooth unstructured meshes. This is particularly important for non-linear waves where the computational mesh has to follow the wave motion using an arbitrary Lagrangian-Eulerian approach.

The approach discussed in this paper was motivated by a detailed stability analysis which indicated that a more direct coupling of the free surface boundary condition with the solution of the Laplace equation significantly enhances numerical stability, without for instance the need to add additional viscosity terms (Ref. [1]) or smoothing (Ref. [3]) to the free surface.

In this paper we will give a brief overview of the main aspects of the numerical discretization, including some theoretical results of the underlying linear scheme. For more details we refer to (Ref. [2]).

Equations governing free surface gravity waves

Consider a time-dependent domain $\Omega(t) \subset \mathbb{R}^3$. We assume that the fluid is incompressible and inviscid, with the velocity field irrotational. The equations of motion for non-linear free-surface gravity waves in a time-dependent reference frame moving with velocity c then can be stated as:

$$-\Delta\phi = 0 \quad \text{in } \Omega(t) \tag{1}$$

together with the free surface boundary conditions at Γ_S:

$$\frac{\partial\phi}{\partial t} + (c + \frac{1}{2}\nabla\phi)\cdot\nabla\phi + \zeta = 0$$
$$\frac{\partial\zeta}{\partial t} + (\overline{c} + \overline{\nabla}\phi)\cdot\overline{\nabla}\zeta - c_3 - \frac{\partial\phi}{\partial x_3} = 0,$$

and a slip flow boundary condition at $\Gamma_N(t)$, which is either a wave maker and/or the bottom of the flow domain:

$$n\cdot\nabla\phi = g_N.$$

Here, ϕ denotes the velocity potential, ζ the wave height, n the unit outward normal vector and g_N a prescribed normal velocity at Γ_N. An overbar refers to only the x_1, x_2 components of a vector $(x_1, x_2, x_3) \in \mathbb{R}^3$, where we assume that $x_3 = 0$ represents the still water surface. In addition, on part of the domain boundary, periodic boundary conditions can be imposed to simulate an unbounded domain. As initial conditions we either start without any waves, with $\phi(x, t_0) = \zeta(x, t_0) = 0$ at Γ_S, and the waves are generated by the wave maker by specifying a periodic normal velocity; or, we start with an analytic wave field in a periodic domain and ϕ, ζ at Γ_S are known at initial time. The equations have been made dimensionless by introducing the water depth H and the gravitational constant g_c as reference quantities.

Discontinuous Galerkin formulation

In this section we summarize the discontinuous Galerkin finite element discretization. The domain Ω is approximated with a tessellation $\mathcal{T}_h$ of shape-regular elements K and the set of all internal faces is represented by $\{\mathcal{F}_h^I\}$. The discontinuous Galerkin finite element discretization uses basis functions which are only weakly coupled to basis functions in neighboring elements. For this purpose, we define the spaces V_h^p and Σ_h^p as:

$$V_h^p := \Big\{ v \in L^2(\Omega) \,\Big|\, v|_K \in \mathcal{P}_p(K),\ \forall K \in \mathcal{T}_h \Big\},$$
$$\Sigma_h^p := \Big\{ \sigma \in [L^2(\Omega)]^3 \,\Big|\, \sigma|_K \in [\mathcal{P}_p(K)]^3,\ \forall K \in \mathcal{T}_h \Big\},$$

with $L^2(\Omega)$ the space of square integrable functions and $\mathcal{P}_p$ the space of polynomials of degree p. For consistency reasons, we need to assume that $\nabla V_h^p \subset \Sigma_h^p$. Since the traces of the functions in V_h^p and Σ_h^p are multi-valued at element faces, we introduce some trace operators in order to define the numerical fluxes in the discontinuous Galerkin formulation. The *average* $\langle v \rangle$ and *jump* $[\![v]\!]$ operators for the trace of $v \in V_h^p$ at an internal face $\mathcal{F} \in \mathcal{F}_h^I$ are defined as:

$$\langle v \rangle := \frac{1}{2}\left(v_L + v_R\right), \qquad [\![v]\!] := v_L n_L + v_R n_R,$$

with $v_L := v|_{\partial K_L}$ and $v_R := v|_{\partial K_R}$, and K_L, K_R the elements connected to the face $\mathcal{F}$ with unit outward normal vectors n_L and n_R, respectively. Similarly, we introduce for the trace of $q \in \Sigma_h^p$ at the face $\mathcal{F} \in \mathcal{F}_h^I$:

$$\langle q \rangle := \frac{1}{2}(q_L + q_R), \qquad [\![q]\!] := q_L \cdot n_L + q_R \cdot n_R,$$

with q_L and q_R analogously defined.

We can now formulate the weak formulation for the potential and wave height of the free surface waves:

Find a $\phi_h, \zeta_h \in V_h^p \times (C^2(t_0,t_n) \cap C^1[t_0,t_n])$, such that for all $v_1, v_2 \in V_h^p$, the following relation is satisfied:

$$B_h^0(\phi_h, v_1) - \Big(\overline{n}\cdot\overline{\nabla}\phi_h, v_1\Big)_{\Gamma_S} - \Big(n_3\frac{\partial \zeta_h}{\partial t}, v_1\Big)_{\Gamma_S} \quad (2)$$
$$- \Big(n_3\big((\overline{c}_h + \overline{\nabla}_h\phi_h)\cdot\overline{\nabla}_h\zeta_h - c_3\big), v_1\Big)_{\Gamma_S} = L_h(v_1)$$
$$\Big(\frac{\partial \phi_h}{\partial t}, v_2\Big)_{\Gamma_S} + \Big(\big(c_h + \frac{1}{2}\nabla_h\phi_h\big)\cdot\nabla\phi_h, v_2\Big)_{\Gamma_S}$$
$$+ \Big(\zeta_h, v_2\Big)_{\Gamma_S} = 0 \quad (3)$$

The operator $B_h^0 : V_h^p \times V_h^p \to \mathbb{R}$ represents the DG discretization of the Laplace equation (1) and is defined as:

$$B_h^0(\phi_h,\psi_h) = \int_\Omega \nabla_h\phi_h\cdot\nabla_h\psi_h dx$$
$$- \sum_{\mathcal{F}\in\mathcal{F}_h^I}\int_{\mathcal{F}}\big([\![\phi_h]\!]\cdot\langle\nabla_h\psi_h\rangle + [\![\psi_h]\!]\cdot\langle\nabla_h\phi_h\rangle\big)ds$$
$$+ \sum_{\mathcal{F}\in\mathcal{F}_h^I}(\eta_{\mathcal{F}} + n_f)\int_\Omega \mathcal{R}_{\mathcal{F}}([\![\phi_h]\!])\cdot\mathcal{R}_{\mathcal{F}}([\![\psi_h]\!])dx,$$

with the *local* lifting operator $\mathcal{R}_{\mathcal{F}} : \left[L^2(\mathcal{F})\right]^d \to \Sigma_h^p$:

$$\int_\Omega \mathcal{R}_{\mathcal{F}}(q)\cdot\sigma dx = \int_{\mathcal{F}} q\cdot\langle\sigma\rangle\, ds \quad \forall\sigma\in\Sigma_h^p.$$

The righthand side of (2) is related to the Neumann boundary condition at Γ_N:

$$L_h(\psi_h) = \int_{\Gamma_N} g_N\psi_h dx.$$

The time derivatives in (3) are approximated with a three-point backward scheme, which results in an unconditionally stable implicit time discretization. The resulting nonlinear equations are solved with a Newton method. With slightly different boundary conditions we can also use the DG discretization for B_h^0 to compute the mesh deformation.

Theoretical results

In a detailed study van der Vegt and Tomar (Ref. [2]) show that the algorithm is unconditionally stable on a general unstructured mesh for linear water waves and does not suffer from a saw-tooth type instability at the free surface. If the coefficient $\eta = \min_{\mathcal{F}\in\mathcal{F}_h^I}\eta_{\mathcal{F}}$ is chosen such that $\eta = \frac{1}{\triangle t}$ then the $L^2(\Gamma_S)$-norm of the error in the wave height is $O(\triangle t^2 + h^{p+1})$, with h the mesh size, $\triangle t$ the time step and p the order of the polynomial basis functions. A similar result holds for the potential function ϕ_h in the $L^2(\Omega)$-norm if the potential function ϕ is sufficiently regular, e.g. $\phi \in H^2(\Omega)$. A discrete Fourier analysis demonstrates that the numerical discretization has a very small numerical dissipation and that the primary error is a dispersion error.

Discussion and results

As an first test for the numerical algorithm we choose a periodic domain with two harmonic modes with different amplitudes and the same periodicity. These two harmonics waves travel across the domain in the same direction but along the opposite diagonals of the rectangular domain. The numerical simulations are done on 3D meshes

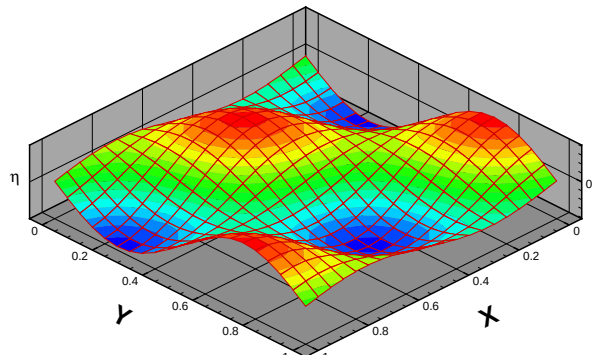

Figure 1: Wave field in three dimensional periodic domain

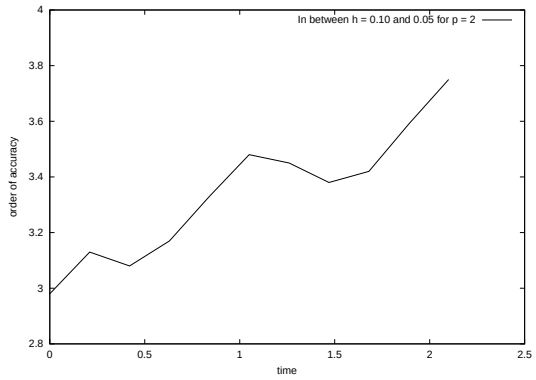

Figure 2: Order of accuracy versus time for 3D harmonic waves.

of size $10 \times 10 \times 5$ and $20 \times 20 \times 10$ for $p = 2$. The free surface profile after one time period is shown in Figure 1. Figure 2 shows that the algorithm is at least third order accurate in space for quadratic basis functions during the simulation.

A second test case is a wave maker in a domain with bump. The domain has a length $L = 4$ and the water depth is normalized to one. In the middle of the domain there is a bump with a height $\frac{3}{4}$ and length 2 and sinusoidal shape. The frequency of the wave maker is 2 and the amplitude is 0.025. For this problem we use three meshes with 20×5, 40×10 and 80×20 elements. In Figure 3 we plot the solution at the different meshes both for linear and quadratic polynomials at $T = 17.5$. These results confirm the theoretical analysis in (Ref. [2]) and show that the algorithms converges quadratic and cubic in the mesh size for $p = 1$ and $p = 2$, respectively, if the time step if sufficiently small. In the full paper we will consider a more extensive set of test cases which exhibit a strong non-linear behavior.

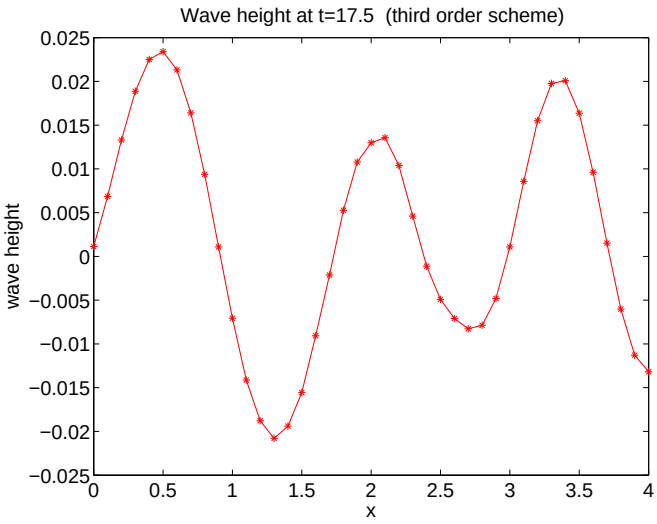

Figure 3: Water waves generated by a wave maker in a domain with a bump for linear ($p = 1$) and quadratic ($p = 2$) polynomials and varying mesh sizes, $h = 0.25, 0.125$ and 0.0625.

Conclusions

An unconditionally stable, implicit higher order accurate discontinuous Galerkin method has been discussed which does not require additional stabilization terms at the free surface to prevent saw tooth type instability at the free surface boundary. The algorithm preserves accuracy on unstructured meshes and is well suited for arbitrary Lagrangian Eulerian techniques using deforming elements. More detailed simulations, including large amplitude waves, will be discussed in the full paper.

Acknowledgement

We would like to acknowledge the collaboration with Dr. S.K. Tomar during the initial development of the DG algorithm. This research was partly funded by the Maritime Research Institute Netherlands (MARIN).

References

[1] Robertson, I., and Sherwin, S.J., (1999). Free-surface flow simulation using *hp*/Spectral elements, *J. Comput, Phys.*, **155**, 26–53.

[2] Van der Vegt, J.J.W. and Tomar, S.K., (2004). Discontinuous Galerkin method for linear free-surface gravity waves, to appear *J. of Sci. Comput.*.

[3] Wu, G.X., and Taylor, R.E., (1994). Finite element analysis of two-dimensional non-linear transient water waves, *Appl. Ocean Res.*, **16**, 363–372.